



# Molecular interaction of an ester-functionalized biodegradable gemini surfactant with lysozyme: Insights from spectroscopy, calorimetry and molecular docking



Mohd. Akram\*, Imtiaz Ahmad Bhat, Sana Anwar, Kabir-ud-Din<sup>1</sup>

Department of Chemistry, Aligarh Muslim University, Aligarh 202002, India

## ARTICLE INFO

### Article history:

Received 5 August 2015

Received in revised form 3 October 2015

Accepted 6 October 2015

Available online 11 November 2015

### Keywords:

16-E2-16

Lysozyme

Quenching

ITC

Docking

## ABSTRACT

Designing and compilation of novel chemical molecules to optimize the structural characteristics of biomolecules is an interesting and fascinating domain of research at the interface of chemistry and molecular biology. In this context, we have synthesized a green/biocompatible gemini surfactant, ethane-1, 2-diyl bis(*N,N*-dimethyl-*N*-hexadecylammoniumacetoxo) dichloride (16-E2-16), and examined its interaction with the model enzyme hen egg white lysozyme (HEWL) utilizing sophisticated spectroscopic, microscopic, calorimetric and molecular modeling techniques. The results obtained through multidimensional approach demonstrate that 16-E2-16 is able to influence the structural aspects of HEWL. The intrinsic fluorescence and UV spectroscopic results reflect HEWL-16-E2-16 complex formation. Synchronous, three-dimensional and pyrene fluorescences show substantial changes in microenvironment around tyrosine and tryptophan residues. CD results demonstrate conformational change in HEWL upon 16-E2-16 combination. ITC suggests the contribution of hydrophobic forces and spontaneous nature of 16-E2-16-HEWL interaction. Molecular modeling confirms the binding of 16-E2-16 gemini surfactant near predominant fluorophores (Trp-62/Trp-108). TEM micrographs infer structural changes in HEWL. This study is thought to have good potential to help scientists to further interpret the surfactant-HEWL interaction at the molecular level, which will be significant to compile surfactant-protein mixtures in general for pharmaceutical and industrial purposes.

© 2015 Elsevier B.V. All rights reserved.

## 1. Introduction

Protein-surfactant interaction is a vital and fascinating concept to understand the conformational, mechanistic and other relevant functional aspects of proteins. Proteins, being the fundamental constituents of life, have characteristic aptitude to bind to inorganic/organic moieties (bilirubin, fatty acids, hematin, metal ions, surfactants, drugs [1–8]). As protein-surfactant combinations are known to induce stabilization/destabilization in the former, these studies are always motivating. In addition, wide scope and significance of protein-surfactant mixtures in biosciences, foods, cosmetics, detergents and biotechnological processes make them even more captivating in the scientific community. In such systems, however, surfactant design is crucial in governing the rhythm of interactions.

The literature survey reveals that most studies regarding protein-surfactant interactions are focused to conventional surfactants [9,10]. Recently, gemini surfactants, bearing two hydrophilic heads and two hydrophobic tails connected covalently through a spacer (at or near the head groups), are receiving considerable interest owing to their

better physicochemical properties than conventional single head/single tail surfactants. They have lower CMC values, much higher surface activity, lower Krafft points, high viscosities at quite low concentrations, etc. [11–13]. They are used as promising surfactants in detergency, gene transfection, ion exchange, vesicle formation, environmental protection, antimicrobial activity, skin/body care products [14], food industry [15], gene delivery [16], drug entrapment/release [17], antimicrobial products [18], etc. Despite these outstanding properties, most of them are non-biodegradable and hence pose environmental concerns. Therefore, cleavable surfactants (conventional as well as gemini) are of keen interest in the scientific community.

The defined cleavable surfactant (16-E2-16) is essential owing to the presence of weak diester (E2) linkage in the spacer. This ester structure makes it biodegradable, cleavable and lowers its CMC (1000 times less than the conventional ones). Thus, 16-E2-16 surfactant is a significant entity to be taken up for further studies.

The monomeric globular protein hen egg white lysozyme (HEWL) contains 129 amino acid residues with four disulfide bonds in its tertiary structure. Its structural architecture involves two domains viz.,  $\alpha$ -domain (1–39 and 89–129 amino acid residues) and  $\beta$ -domain (40–88 amino acid residues [19,20]). It possesses a rigid structure [21] and has six Trp residues arranged, respectively, at active site (3 residues), hydrophobic core (two residues) and separate (one residue).

\* Corresponding author.

E-mail address: [drmohdakram@rediff.com](mailto:drmohdakram@rediff.com) (M. Akram).

<sup>1</sup> Present address: Department of Chemistry, Arba Minch University, Ethiopia.

The predominant fluorescence of lysozyme is mainly due to the Trp 62 and Trp 108 fluorophores [22].

In this work we have examined the molecular interaction of ester-functionalized green/biocompatible gemini surfactant, ethane-1, 2-diyl bis(*N,N*-dimethyl-*N*-hexadecylammoniumacetoxyl) dichloride (16-E2-16) with HEWL. Lysozyme was chosen owing to its physiological and pharmaceutical properties. Moreover, in our recent studies, 16-E2-16 surfactant was observed to be quite effective in modulating BSA fibrils [23]. Therefore, we believe that HEWL-16-E2-16 interaction too will serve the means to further interpret heredity-systematic amyloidosis disease (in vitro) by taking HEWL as model. Other reason being the structural homology of HEWL with human lysozyme and both form quite similar fibrils [24,25].

Keeping the above facts in consideration, we can conclude that this study can be significant in biomedical, pharmaceutical and industrial (cosmetics, food and feed) realms at molecular level.

## 2. Materials and methods

### 2.1. Materials

Chloroacetyl chloride (98%, Loba-Chemie, India), ethylene glycol (99%, Sigma Aldrich, USA), *N,N*-dimethylhexadecylamine (95%, Sigma Aldrich, USA), hen egg white lysozyme (HEWL, Sigma Aldrich, USA), and pyrene (98%, Acros Organics, Belgium) were used as received. The gemini surfactant, ethane-1,2-diyl bis(*N,N*-dimethyl-*N*-hexadecylammoniumacetoxyl) dichloride (16-E2-16), was synthesized following

the literature procedure [26–29]. The synthesis protocol is shown in Scheme 1. Working solution concentrations were: [HEWL] =  $20 \times 10^{-6}$  M, [PB] =  $12 \times 10^{-3}$  M, pH = 7.4.

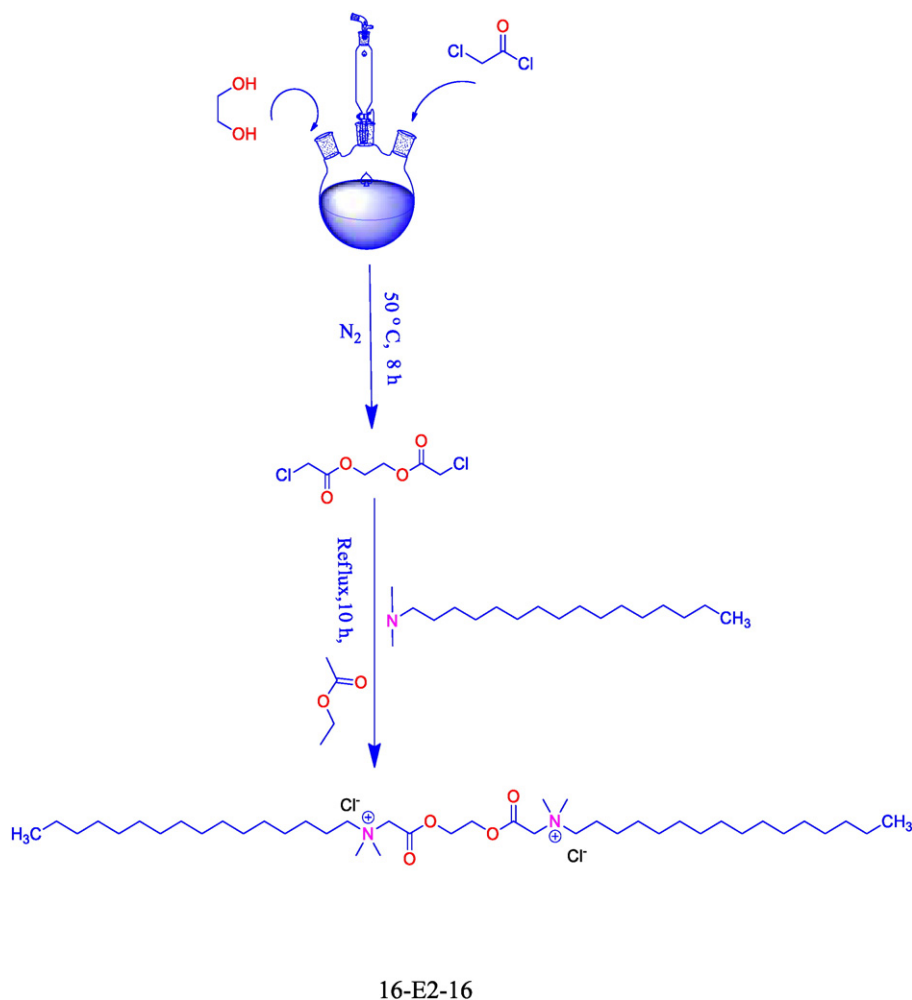
### 2.2. Methods

#### 2.2.1. Spectroscopic measurements

The steady-state fluorescence spectra were obtained using a Hitachi F-2700 fluorescence spectrophotometer (Japan), equipped with a PC. Prior to experiment, the instrument parameters were set as: excitation wavelength (280 nm), emission wavelength range (300–450 nm), and slit width (5 nm). Three-dimensional fluorescence was recorded in the range of 250–600 nm, keeping other parameters relevant to steady-state fluorescence. Synchronous fluorescence spectra were observed from the same instrument keeping  $\Delta\lambda$  between the excitation and emission wavelengths equal to 20 and 60 nm, respectively. For observation of extrinsic fluorescence spectra, excitation wavelength was kept at 337 nm and emission spectra were recorded in the range of 350–450 nm. For UV absorption spectra recording (200–330 nm), Perkin Elmer Lambda-25 (Singapore) was used. CD measurements were performed on Jasco-J-815 spectropolarimeter with instrument parameters as: temperature (298 K), scan range (200–250 nm), scan speed (100 nm/min), and response time (1 s).

#### 2.2.2. ITC measurements

Isothermal titration calorimetry was performed using a Microcal ITC-200 Calorimeter (USA). Gemini surfactant titrants were dissolved



Scheme 1. Protocol for 16-E2-16 gemini surfactant synthesis.

in the 12 mM PB (pH 7.4). 20  $\mu$ M HEWL samples were placed in the reaction cell, and the reference cell was filled with the buffer. All titrations were performed at 298 K. After temperature equilibration, the titrant was injected sequentially in 2  $\mu$ l aliquots increments at 120 s interval with stirring at 500 rpm to ensure a complete equilibration. The resulting heats of reaction were measured upto 19 consecutive injections.

### 2.2.3. Molecular modeling measurements

Molecular modeling was performed by using molecular graphics program HEX 6.1 [30]. The PDB (1 DPX) of HEWL was downloaded from the protein data bank and PDB files of 16-E2-16 surfactant were developed by using Chimera 1.9 and visualization of docked conformation was achieved by using Pymol [31]. The docking experiment was run on computer using Windows 7 as an operating system.

### 2.2.4. TEM measurements

Transmission electron microscopy was performed on a JEM-2100 (JEOL, Japan) electron microscope. The samples of HEWL and HEWL + 16-E2-16 were prepared by negative staining method [32, 33]. Then TEM photos were pictured after thorough drying of the samples.

## 3. Results and discussion

### 3.1. Fluorescence quenching of HEWL by 16-E2-16 and the binding mechanism analysis

Steady-state fluorescence is an effective method to study interactions between small molecules and proteins. Fig. 1 (a) shows the fluorescence spectra of HEWL with increasing concentration of 16-E2-16 gemini surfactant which reveals quenching of fluorescence intensity of HEWL with slight blue shift ( $\sim 3$  nm). This behavior may be attributed to the HEWL-16-E2-16 complex formation and an exposure of aromatic residues (mainly Trp/Tyr) to a non-polar environment.

Fluorescence quenching usually proceeds through two mechanisms: static and the dynamic. The static mechanism involves the formation of ground state complex between fluorophore and quencher while dynamic quenching proceeds through the formation of excited state complex. A better understanding of the quenching mechanism can be reached from quantitative analysis of the experimental data. One such method involves the application of Stern–Volmer Eq. (1)

$$\frac{F_0}{F} = 1 + K_{SV}[Q] \quad (1)$$

where  $F_0$  and  $F$  represent the fluorescence intensities in the absence and presence of quencher,  $[Q]$  and  $K_{SV}$ , respectively, indicate the quencher

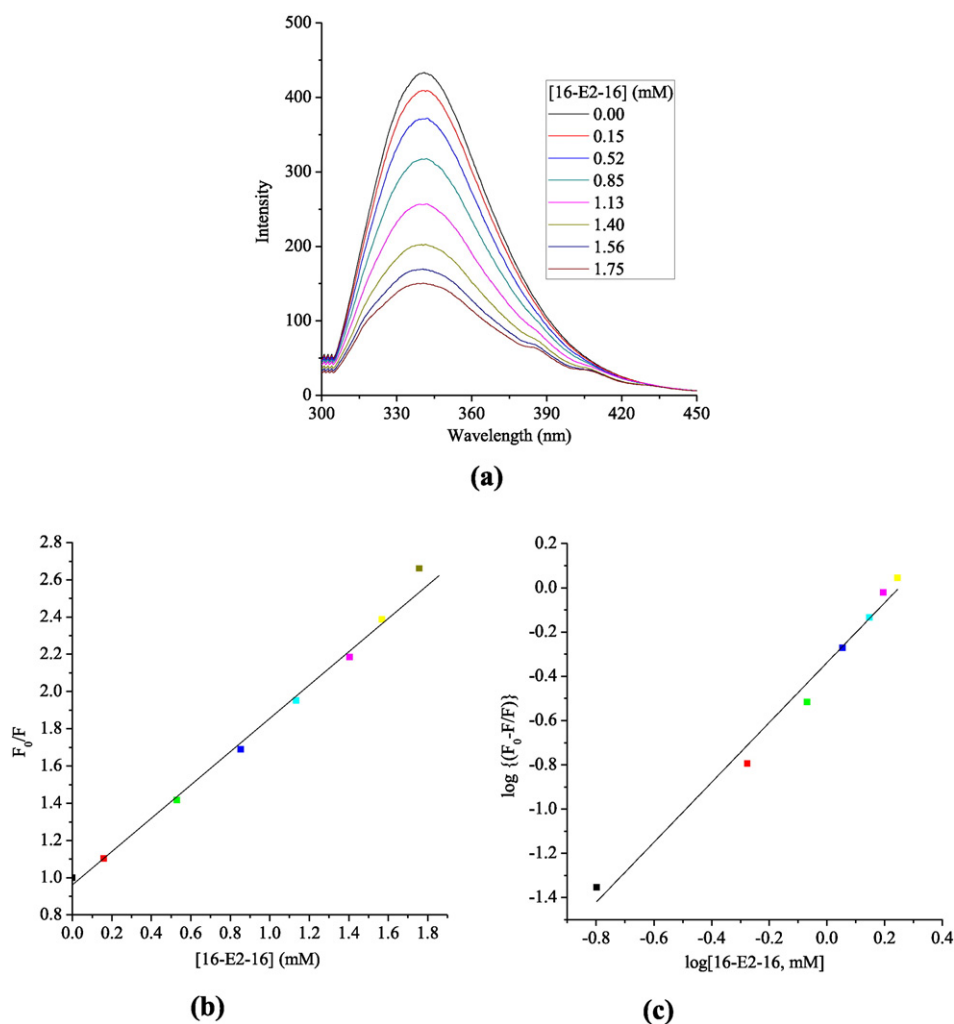


**Fig. 1.** The fluorescence quenching results of the lysozyme HEWL/16-E2-16 gemini surfactant system: (a) quenching profiles with varying concentrations of the surfactant, (b) the Stern–Volmer plot, and (c) the modified Stern–Volmer plot.

concentration and the Stern–Volmer quenching constant. The  $K_{SV}$  ( $8.8 \times 10^4 \text{ L mol}^{-1}$ ), obtained from slope of Fig. 1 (b), reveals substantial quenching of the emission spectra of HEWL by 16-E2-16. The  $K_{SV}$  value was then utilized to obtain quenching rate constant ( $k_q$ ) from the following equation

$$k_q = \frac{K_{SV}}{\tau_0} \quad (2)$$

Here,  $\tau_0$  is the life time of the fluorophore and is  $10^{-8} \text{ s}$  for biomolecules [34]. Magnitude of the evaluated  $k_q$  ( $8.8 \times 10^{12} \text{ L mol}^{-1} \text{ s}^{-1}$ ) is greater than the scatter constant ( $2 \times 10^{10} \text{ L mol}^{-1} \text{ s}^{-1}$  [35]). Therefore, it can be concluded that the quenching proceeds by means of static procedure rather than dynamic and involves the ground state complex formation between 16-E2-16 and HEWL. Moreover, to compute the binding constant ( $K_b$ ) and number of binding sites, the modified Stern–Volmer Eq. (3) was used. The antilog of intercept ( $\log K_b$ ) and

slope ( $n$ ) of plot (Fig. 1 (c)) were used to compute the binding constant and number of binding sites, respectively

$$\log\{(F_0 - F/F)\} = \log K_b + n \log[16\text{-E2-16}] \quad (3)$$

The obtained value of binding constant ( $K_b = 6.3 \times 10^4 \text{ L mol}^{-1}$ ) is significant which discloses convincing binding of 16-E2-16 to HEWL and the value of  $n = 1.48$  infers the single pattern of binding sites on HEWL. Further, binding process was observed to be spontaneous and thermodynamically favored as the  $\Delta G_b^\circ$  value (obtained by employing equation  $\Delta G_b^\circ = -RT \ln K_b$ ) was found to be negative ( $-6.55 \text{ kcal mol}^{-1}$ ).

Further authentication to HEWL-16-E2-16 complex formation was provided by three-dimensional fluorescence. It gives reliable information about the microenvironment changes around aromatic residues. Fig. 2 (a–b) represents the relevant spectra of HEWL in the absence and presence of 16-E2-16. It can be seen that HEWL displays two

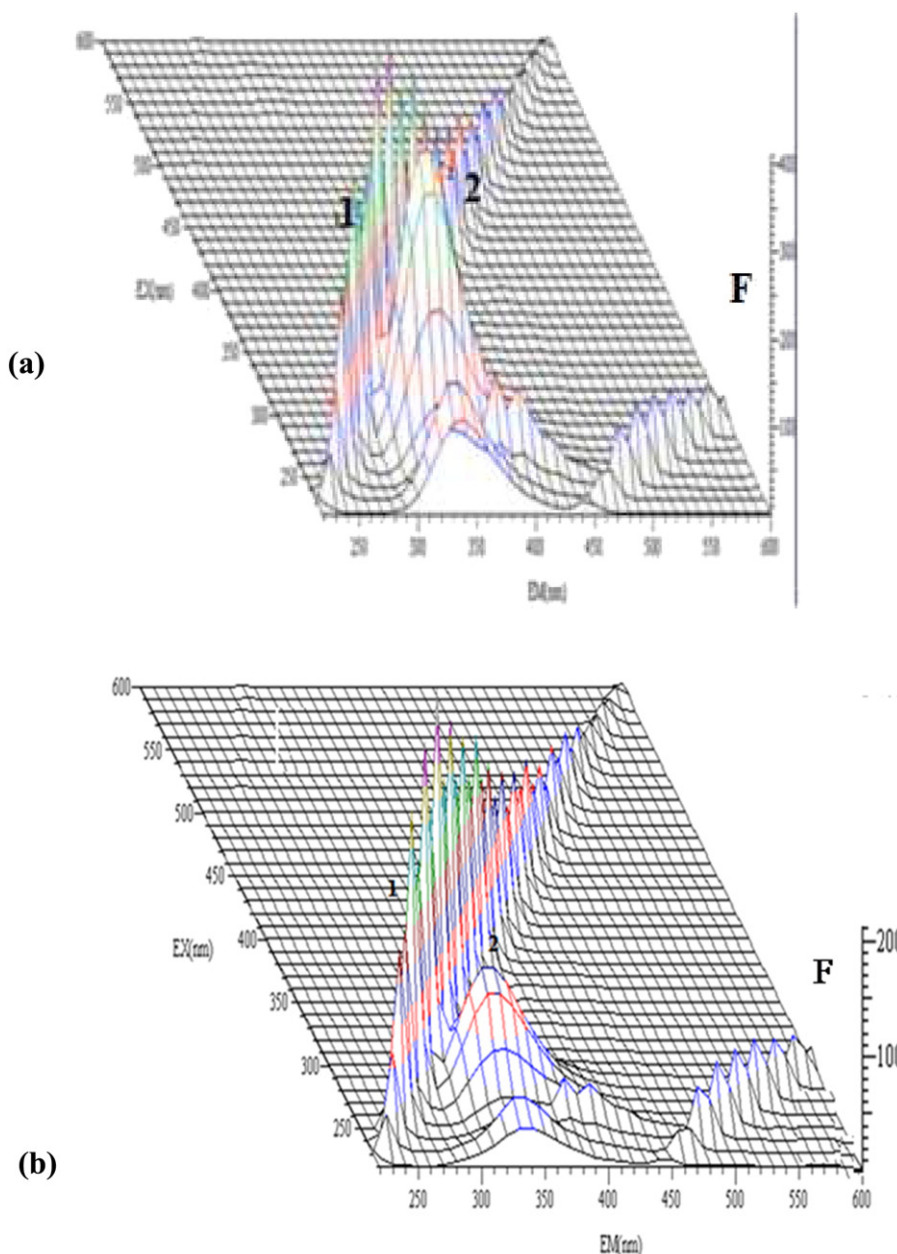


Fig. 2. Three-dimensional fluorescence spectra of lysozyme (HEWL) in the absence (a), and presence (b) of 16-E2-16 gemini surfactant.

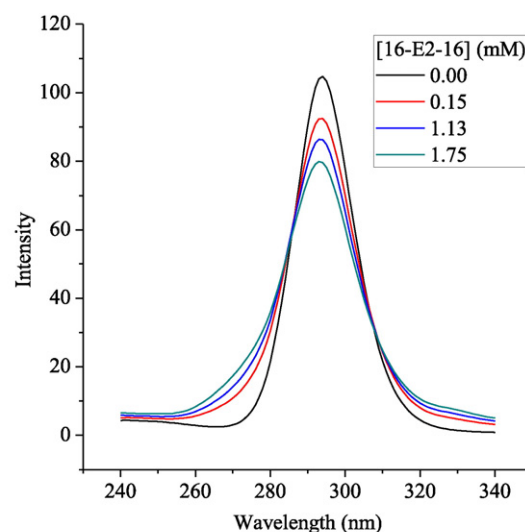
peaks. Peak 1 corresponds to Rayleigh scattering and peak 2 is a contribution from the aromatic residues (Tyr/Trp). Fig. 2(b) shows that the 16-E2-16 addition leads to decrease in the fluorescence intensity of the aromatic residue peak, which infers distinct change in the molecular microenvironment in the vicinity of Tyr/Trp-residues. The reason for this quenching can be attributed to the higher chain length of 16-E2-16. Higher chain length lets 16-E2-16 to form micelles quite readily, consequently leading to an extended structure of HEWL with exposed hydrophobic patches. The quenching of fluorescence peak can also be explained by assuming HEWL anion with considerable negative sites. This negatively charged surface of HEWL interacts with the positively charged head groups of 16-E2-16 gemini surfactant, which favors mitigation of the electrostatic repulsions; this enhances the aggregation of 16-E2-16 moieties on to the protein surface and hence produce quenching.

### 3.2. Synchronous fluorescence

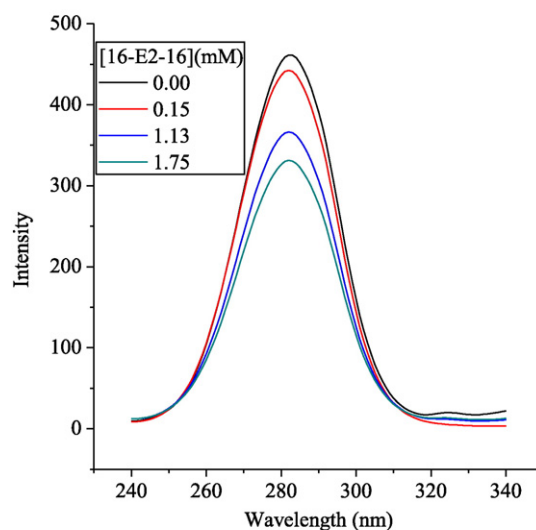
Microenvironment fluctuation around fluorophores (Tyr/Trp) was also monitored by synchronous fluorescence. As compared to conventional fluorescence, synchronous fluorescence is considered suitable due to its specificity towards aromatic residues. It also mitigates spectral overlaps by thinning spectral bands and simplifies spectra by using an appropriate wavelength [36]. Keeping the  $\Delta\lambda$  between the excitation and emission wavelengths at 20 and 60 nm, respectively, microenvironment changes around tyrosine and tryptophan residues can be probed [36]. The relevant synchronous fluorescence spectra (Fig. 3(a–b)) reveal that addition of 16-E2-16 gemini surfactant produces quenching around both the fluorophores (Tyr or Trp), indicating the interaction and complexation of 16-E2-16 with HEWL. This quenching in fluorescence is due to an exposure of an aromatic residue to hydrophobic tail of 16-E2-16. Interactions are more effectively evident in Fig. 3(b) than in Fig. 3(a); the reason being a higher affinity of 16-E2-16 molecules towards tryptophan (Trp) than tyrosine (Tyr) residue. This fact is in coherence with the results obtained in steady-state fluorescence.

### 3.3. Pyrene fluorescence and micropolarity assay

To add further confirmation to the fact that there is a structural change in HEWL upon 16-E2-16 gemini surfactant combination, pyrene, an extrinsic fluorescent probe, was utilized. Pyrene excites at 337 nm and has characteristic five peak vibronic spectra (Fig. 4 (a)) in the scan range of 350–450 nm. It is interesting to note that in the absence of gemini surfactant, the fluorescence peak is having low intensity (Fig. 4 (a)), suggesting the occurrence of pyrene in the hydrophobic domains of HEWL. The addition of 16-E2-16 gemini surfactant leads to an increase in the fluorescence intensity (Fig. 4 (a)), depicting an exposure of buried hydrophobic patches of HEWL to a non-polar environment exerted by the surfactant. After few additions, the fluorescence intensity starts diminishing (Fig. 4 (a)), which indicates migration of the probe molecules into the 16-E2-16 microstructures. Moreover, the local polarity index ( $F_1/F_3$  ratio) of the protein solution was also monitored and calculated from the first and third vibronic peaks of pyrene [32]. The results are shown in Fig. 4 (b). A careful observation of Fig. 4 (b) reveals that the HEWL solution has a lower  $F_1/F_3$  value, which again confirms the localization of pyrene in the hydrophobic network. Subsequent additions of 16-E2-16 lead to an increase in the  $F_1/F_3$  ratio, followed by near constancy at higher concentrations of the surfactant. The increasing trend can be attributed to the enzyme unfolding, and the unchanging micropolarity at higher concentrations can be assigned to abundant aggregate microstructures formed by the 16-E2-16 gemini surfactant. Thus, from the micropolarity assay, we can conclude that there are substantial structural changes in the HEWL solution upon gemini surfactant combination.



(a)



(b)

**Fig. 3.** Synchronous spectra of HEWL in the presence of varying concentrations of 16-E2-16 at 298 K (a)  $\Delta\lambda = 20$  nm (represents contributions due to tyrosine), and (b)  $\Delta\lambda = 60$  nm (represents contributions due to tryptophan).

### 3.4. Far-UV circular dichroism analysis

To further validate and support the above findings concerning the effect of 16-E2-16 gemini surfactant on the secondary structure of HEWL, circular dichroism (CD) studies were performed. CD is regarded as a very consistent technique to authenticate the conformational changes in proteins [37,38]. The CD spectra of HEWL in presence of different concentrations of 16-E2-16 gemini surfactant are given in Fig. 5. The spectra show two characterized  $\alpha$ -helix negative peaks, respectively, at 220 and 208 nm. Subsequent addition of 16-E2-16 leads to decrease in the negative ellipticity, inferring the structural change in HEWL. The quantitative estimation of percentage of  $\alpha$ -helicity was obtained by converting the obtained CD data into mean residue ellipticity (MRE), by employing the following equation

$$\text{MRE} = \frac{\text{Observed CD (m degree)}}{C_p n l \times 10} \quad (4)$$

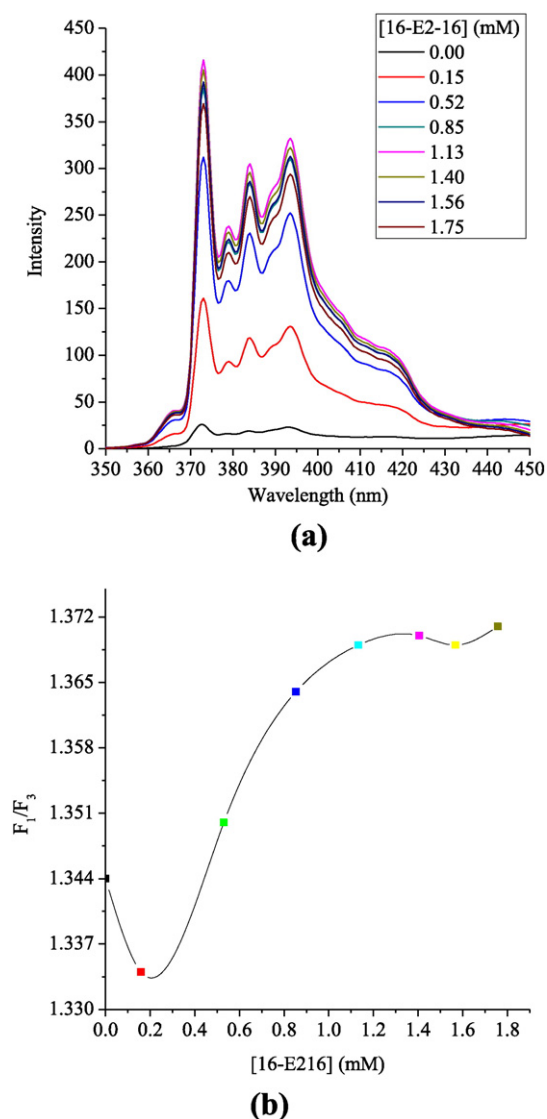


**Fig. 4.** (a) Pyrene emission spectra of lysozyme (HEWL) in the presence of varying amounts of 16-E2-16 surfactant, and (b) variation of  $F_1/F_3$  ratio with the 16-E2-16 surfactant concentration.

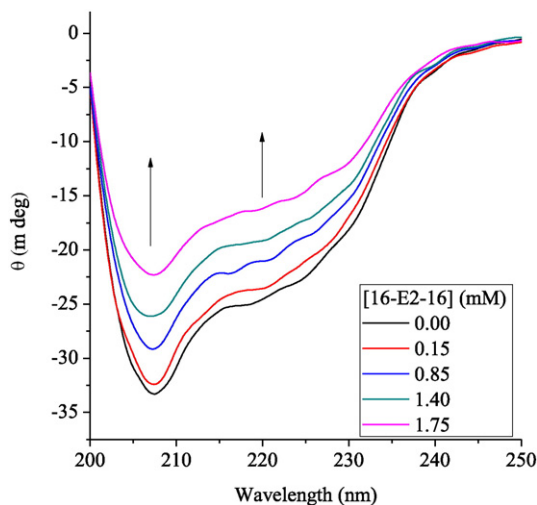


**Fig. 5.** Far UV-CD spectra of lysozyme (HEWL) in the presence of varying amounts of 16-E2-16 surfactant.

where  $C_p$ ,  $n$  and  $l$ , respectively, represent the molar concentration of protein, number of amino acid residues (129 in HEWL) and path-length (1 mm). The  $\alpha$ -helical content of free and combined systems of HEWL from MRE values (at  $\theta = 208$  nm) were then calculated by employing the following equation [39] and the results obtained are listed in Table 1

$$\alpha\text{-Helix (\%)} = \frac{\text{MRE}_{208} - 4000}{33,000 - 4000} \times 100. \quad (5)$$

It can be observed from Table 1 that the addition of gemini surfactant leads to a reduction in the negative helicity, indicating that the binding of 16-E2-16 gemini surfactant to HEWL induces change in the secondary structure. At low surfactant concentration, there is little change in the helicity but, at higher surfactant concentration, helicity decreases appreciably. The reason for this structural change can be attributed to preferential adsorption (at high surfactant concentration) of 16-E2-16 molecules on the HEWL surface which leads to a sort of bulging of the enzyme; this, in turn, exposes the hydrophobic residues and ultimately  $\alpha$ -helices are broken to give a more open disordered structure. Thus, we conclude that gemini surfactant at higher concentration disrupts the  $\alpha$ -helical network and leads to a more open, random, solvent-exposed protein structure. This indicates significant perturbation of the surface tryptophan and tyrosyl residues. Thus, 16-E2-16 gemini surfactant perturbs the structure of the protein surface, mediating the water layer and microenvironment around the superficial aromatic residues. This finding also supports the fluorescence quenching of tryptophan and tyrosyl residues upon their exposure to the outer environment. Thus, our fluorescence results are in corroboration with the CD results.

### 3.5. UV-visible study

UV-visible absorption studies are widely applied to analyze the structural changes and complex formation between ligands and proteins. The absorbance at 280 nm is due to the aromatic residues (Trp or Tyr) of HEWL and is a sensitive parameter to confirm the micropolarity changes as well as complex formation between ligand and enzyme. This absorbance is mainly attributed to  $\pi-\pi^*$  transitions of aromatic residues. Fig. 6 shows the absorption spectra of HEWL with increasing concentration of 16-E2-16 gemini surfactant. Clearly, the absorbance at 280 nm decreases with an increase in the concentration of 16-E2-16. This decrease in absorbance infers the change in the microenvironment around aromatic residues [40] and reflects the inducement of structural change thereupon. A careful observation of the spectra also indicates the presence of slight blue shift ( $\sim 5$  nm), inferring an exposure of hydrophobic residues to the outer environment. In other words, we can conclude that binding of the 16-E2-16 gemini surfactant to HEWL induces unfolding in the latter.

### 3.6. Isothermal titration calorimetry (ITC)

ITC is an interesting and novel approach to validate interactions between proteins and ligands. Its multidimensional approach makes it even more attractive and appropriate for protein/drug/surfactant interactions. The ITC titration profile of HEWL with different molar ratios of 16-E2-16 is shown in Fig. 7. Each peak in the thermogram

**Table 1**  
Variation of  $\alpha$ -helical content of HEWL as function of 16-E2-16 concentration.

[16-E2-16] (mM)	$\alpha$ -Helix (%)
0	30.68
0.15	29.79
0.85	25.11
1.40	20.90
1.75	15.86

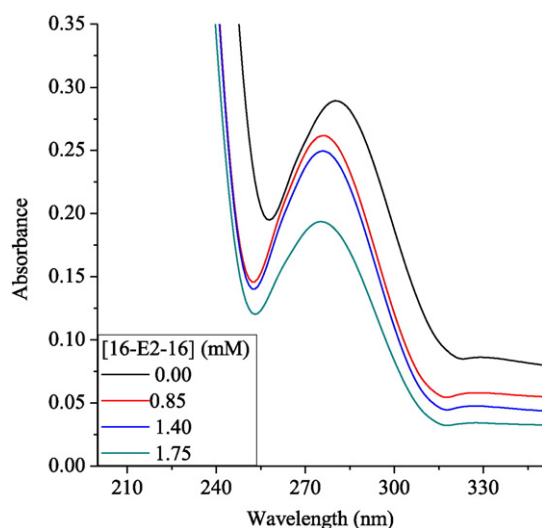


Fig. 6. Absorption spectra of lysozyme (HEWL) with varying amounts of 16-E2-16 surfactant.

(upper panel) represents a single injection of 16-E2-16 into the HEWL solution. All the peaks are upward, indicating that reactions mainly proceed through endothermic event. The integrated and normalized patterns are shown in Fig. 7 (lower panel). It is evident from Fig. 7 (lower panel) that the consecutive additions of 16-E2-16 gemini surfactant in to HEWL solution induce reduction in the endothermicity which evidences the interaction of 16-E2-16 with HEWL. Careful observation of the Fig. 7 (lower panel) reveals that all the observed enthalpy values are positive, suggesting rupture of hydrogen bonding [41] during the HEWL and 16-E2-16 interactions. The reason for this structural reorientation are hydrophobic interactions [42], which are supposed to induce random arrangement of solvent molecules during the interaction. Moreover, the obtained calorimetric data are given in Table 2. It is interesting to note from Table 2 that  $\Delta H^\circ$  and  $\Delta S^\circ$  are positive, indicating that van der Waals forces are not operating in the 16-E2-16-HEWL system and predominance of hydrophobic interactions. Further,  $\Delta G_b^\circ$  value are found to be negative, indicating interaction of 16-E2-16 with HEWL is spontaneous. This fact is in coherence with our fluorescence results, in which we have also obtained negative value of  $\Delta G_b^\circ$ . However, on comparing the magnitude of calorimetric parameters with fluorescence binding it is clear that in ITC  $K_b$  as well  $\Delta G_b^\circ$  are found higher in magnitude than the fluorescence, reason being ITC measures the global change (i.e. enthalpy change of the binding reaction as well as the enthalpy of all possible concomitant reactions which may accompany the binding reactions but not directly influence the  $K_b$ ) while as fluorescence is specific to aromatic residues [43]. Further the obtained binding stoichiometry in ITC suggests the possibility of two binding sites which is different from one binding site approximation of fluorescence. This may be due to absence of tryptophan residue in the close vicinity of binding event captured by fluorescence. Other reason for higher values of binding parameters obtained in ITC may be attributed to long chain length of 16-E2-16, as it is known that longer chains (with 16–22 carbon number) can alter  $K_b$  values strongly [44].

### 3.7. Computational molecular docking

Molecular docking is an attractive computational tool to ascertain and validate the probable interactions of small molecules with biomacromolecules [45], which has rational significance in molecular recognition and drug design related phenomenon. Therefore, computational molecular docking was performed to examine the binding loci of 16-E2-16 gemini surfactant in the HEWL. The stereo docked pose of 16-E2-16 + HEWL (Fig. 8(a)) reveals that 16-E2-16 binds in the vicinity of Trp-111, Val-109, Trp-108, Ala-107, Trp-62, Trp-63, Ser-60, Cys-64,

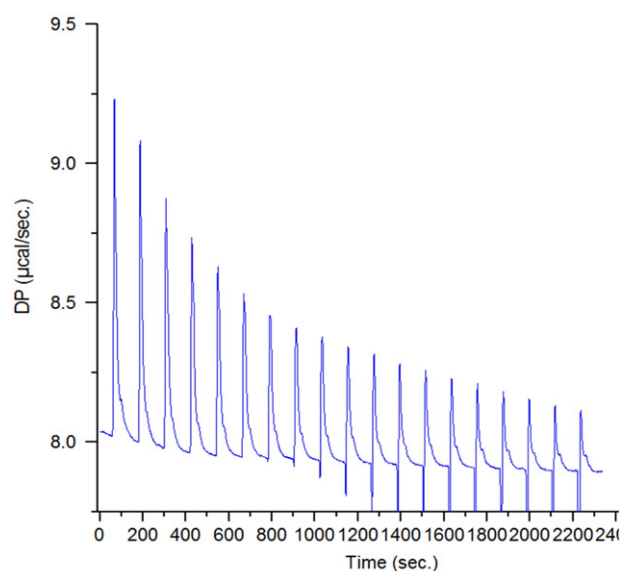
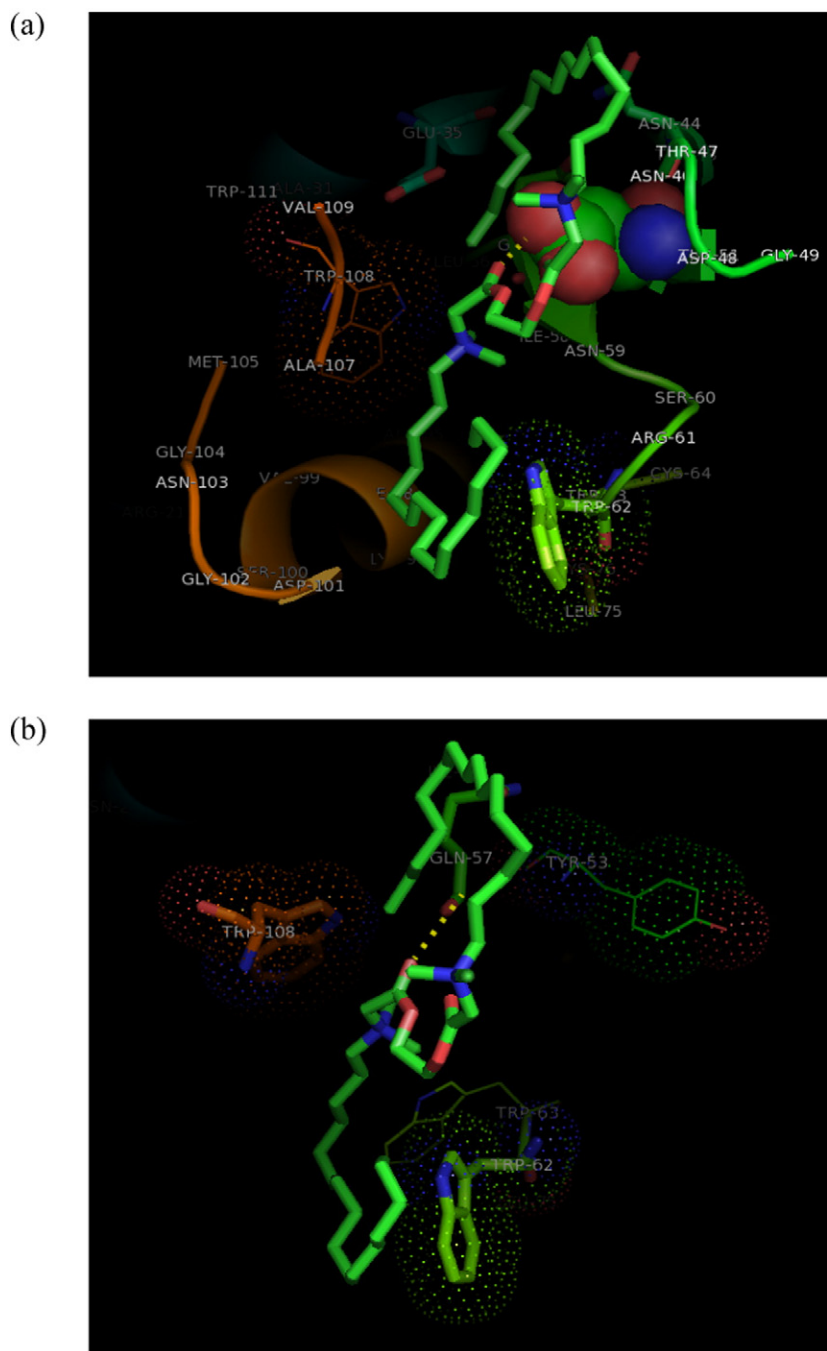


Fig. 7. ITC profiles for binding of 16-E2-16 gemini surfactant to lysozyme (HEWL) at 298 K.

Arg-6, Gln-57, Glu-35, Asn-44, Thr-44, Ser-36, Asp-52, amino acid residues. It can be seen (Fig. 8 (b)) that 16-E2-16 gemini surfactant accommodates itself in the locality of Trp-108, Trp-62 and Trp-63 residues. This observation supports the fluorescence quenching. Interestingly,

**Table 2**  
ITC derived biophysical parameters for the binding of 16-E2-16 with HEWL at 298 K and pH 7.4.

16-E2-16-HEWL	
n	2.6
$K_b$	$5.6 \times 10^{14} \text{ M}^{-1}$
$\Delta H^\circ$	350.2 cal/mol
$\Delta S^\circ$	68.7 cal/mol/deg
$\Delta G_b^\circ$	−20.13 kcal/mol



**Fig. 8.** Docked pose of 16-E2-16 (a) in the binding site of lysozyme HEWL, and (b) shown in the close vicinity of Trp 62, Trp-63, Trp-108 and Tyr-53 aromatic residues.

the presence of 16-E2-16 gemini in hydrophobic residues infers that hydrophobic forces mainly govern the binding process. Further, possibility of hydrogen bonding interactions in the glutamine (Gln-57) and the oxygen of the ester moiety of 16-E2-16 gemini is also evident in docking results. The significant binding interaction energy ( $-320.44 \text{ kJ mol}^{-1}$ ) also unveils considerable interaction between 16-E2-16 and HEWL. Here, it is also interesting to note that magnitude of binding interaction energy is different from fluorescence and ITC energy magnitudes; it is due to exclusion of solvent during docking experiment.

### 3.8. Transmission electron microscopy

Further validation to our overall results were added by transmission electron microscopy (TEM). The aggregated globular structures (Fig. 9(b)) were observed in mixed systems (16-E2-16 + HEWL). No

such forms were observed in untreated native HEWL (Fig. 9(a)). The predominance of electrostatic repulsion at higher surfactant concentrations were found to be attributive. Moreover, our overall results further get support from the literature [46].

## 4. Conclusion

In this research article we have investigated the interaction of an ester-functionalized green/biocompatible gemini surfactant, ethane-1, 2-diyl bis(*N,N*-dimethyl-*N*-hexadecylammoniumacetoxo) dichloride (16-E2-16), with HEWL by employing fluorescence, absorption spectroscopy (UV), circular dichroism, ITC, TEM and molecular modeling. The results obtained through various spectroscopic approaches delineate that the biodegradable gemini surfactant effectively interacts with the HEWL and causes structural alteration in the latter. Various

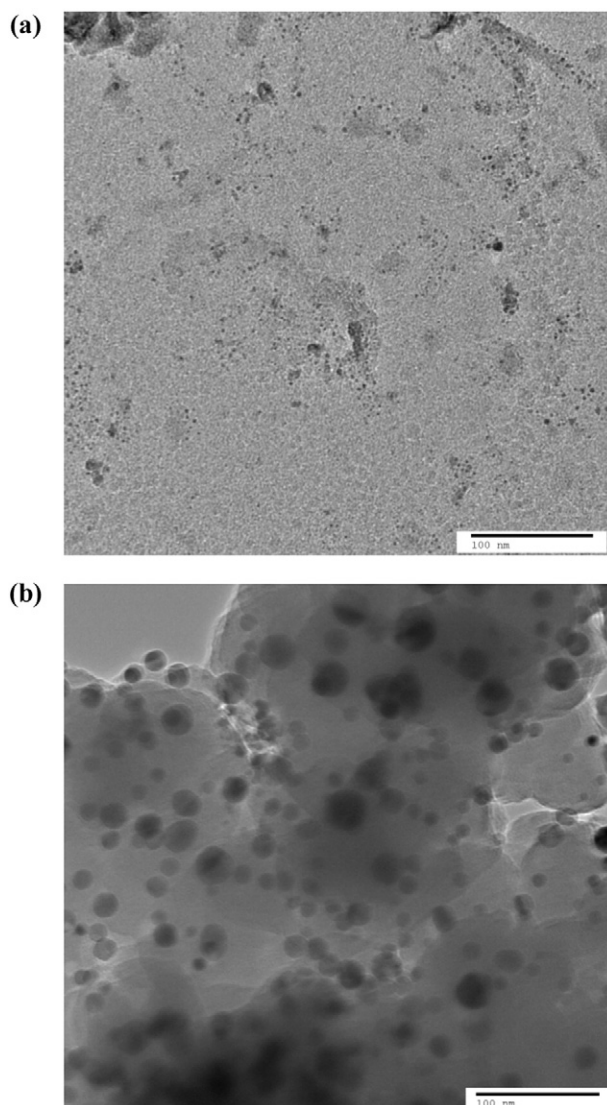


Fig. 9. TEM micrographs of (a) HEWL, and (b) HEWL + 16-E2-16.

biophysical binding parameters infer that quenching of fluorescence spectra proceeds through static pathway rather than dynamic one. CD results depict conformational alteration upon gemini combination. Appearance of globular aggregated structures in transmission electron microscopy results (TEM) validates the structural change in HEWL and 16-E2-16–HEWL complex formation. Molecular docking provides insight that 16-E2-16 binds near to predominant fluorophores, Trp-108 and Trp-62. This accounts for predominant hydrophobic forces governing the interaction, which is in well coherence with ITC results in which a single endothermic event was also observed. Positive values of  $\Delta S^\circ$  and  $\Delta H^\circ$  infer the predominance of hydrophobic interactions during 16-E2-16 and HEWL interaction. Moreover, negative  $\Delta G_b^\circ$  value obtained in ITC suggests the spontaneous nature of concerned interactions as was indicated by fluorescence and docking studies.

This study will be significant in understanding the protein–surfactant interaction at the molecular level and assumes importance in the biomedical and pharmaceutical world.

#### Acknowledgments

IAB gratefully acknowledges the University Grants Commission, New Delhi, India for BSR (Basic Science Research) fellowship. We are

also thankful to the USIF (University Sophisticated Instruments Facility), Aligarh Muslim University, for providing TEM (Transmission Electron Microscopy) facility.

#### References

- [1] A. Sułkowska, B. Bojko, J. Równicka, D. Pentak, W. Sułkowski, *J. Mol. Struct.* 651–653 (2003) 237–243.
- [2] S. De, A. Girigoswami, S. Das, *J. Colloid Interface Sci.* 285 (2005) 562–573.
- [3] D. Kelley, D.J. McClements, *J. Food Hydrocoll.* 17 (2003) 73–85.
- [4] M. Vasilescu, D. Angelescu, M. Almgren, A. Valstar, *Langmuir* 15 (1999) 2635–2643.
- [5] B.P. Kamat, J. Seetharamappa, *J. Pharm. Biomed. Anal.* 35 (2004) 655–664.
- [6] H. Bai, X. Liu, Z. Zhang, S. Dong, *Spectrochim. Acta A* 60 (2004) 155–160.
- [7] B. Farruggia, B. Nerli, H.D. Nuci, R. Rigatusso, G. Picó, *Int. J. Biol. Macromol.* 26 (1999) 23–33.
- [8] A. Sułkowska, *J. Mol. Struct.* 614 (2002) 227–232.
- [9] N.J. Turro, X.G. Lei, K.P. Ananthapadmanabhan, M. Aronson, *Langmuir* 11 (1995) 2525–2533.
- [10] S. Ghosh, A. Banerjee, *Biomacromolecules* 3 (2002) 9–16.
- [11] F.M. Menger, C.A. Littau, *J. Am. Chem. Soc.* 113 (1991) 1451–1452.
- [12] R. Zana, *J. Colloid Interface Sci.* 248 (2002) 203–220.
- [13] M.J. Rosen, *Surfactants and Interfacial Phenomenon*, 3rd ed. John Wiley and Sons, New York, 2004.
- [14] M. Macián, J. Seguer, M.R. Infante, C. Selve, M.P. Vinardell, *Toxicology* 106 (1996) 1–9.
- [15] R. Zana, J. Xia, *Gemini Surfactants: Synthesis, Interfacial and Solution-Phase Behavior and Applications Surfactant Science Series*, vol. 117, Marcel Dekker, Inc., New York, 2004.
- [16] A. Bajaj, B. Paul, S.S. Indi, P. Kondaiah, S. Bhattacharya, *Bioconjug. Chem.* 18 (2007) 2144–2158.
- [17] C. Bombelli, G. Caracciolo, P.D. Profio, M. Diociaiuti, P. Luciani, G. Mancini, C. Mazza, M. Marra, A. Molinari, D. Monti, L. Toccaceli, M. Venanzi, *J. Med. Chem.* 48 (2005) 4882–4891.
- [18] L. Caillier, E.T.D. Givenchy, R. Levy, Y. Vandenberghe, S. Geribaldi, F. Guittard, *J. Colloid Interface Sci.* 332 (2009) 201–207.
- [19] M.C. Vaney, S. Maignan, M.R. Kautt, A. Ducriux, *Acta Crystallogr. Sect. D: Biol. Crystallogr.* 52 (1996) 505–517.
- [20] M.B. Pepys, P.N. Hawkins, D.R. Booth, D.M. Vigushin, G.A. Tennent, A.K. Soutar, N. Totty, O. Nguyen, C.C.F. Blake, C.J. Terry, T.G. Feest, A.M. Zalin, J.J. Hsuan, *Nature* 362 (1993) 553–557.
- [21] C.C.F. Blake, D.F. Koenig, G.A. Mair, A.C.T. North, D.C. Phillips, V.R. Sarma, *Nature* 206 (1965) 757–761.
- [22] T. Imoto, L.S. Foster, J.A. Ruoley, F. Tanaka, *Proc. Natl. Acad. Sci. U. S. A.* 69 (1972) 1151–1155.
- [23] Z. Yaseen, S. Rehman, M. Tabish, A.H. Shalla, Kabir-ud-Din, *RSC Adv.* 5 (2015) 58616–58624.
- [24] L.N. Arnaudov, R. de Vries, *Biophys. J.* 88 (2005) 515–526.
- [25] L.A. Morozova-Roche, J. Zurdo, A. Spencer, W. Noppe, V. Receveur, D.B. Archer, M. Joniau, C.M. Dobson, *J. Struct. Biol.* 130 (2000) 339–351.
- [26] G. Zhihong, T. Shuxin, Z. Qi, Z. Yu, L. Bo, G. Yushu, H. Li, T. Xiaoyan, *Wuhan Univ. J. Nat. Sci.* 13 (2008) 227–231.
- [27] M. Akram, I.A. Bhat, Z. Yaseen, Kabir-ud-Din, *Colloids Surf. A* 444 (2014) 209–216.
- [28] M. Akram, I.A. Bhat, Kabir-ud-Din, *J. Phys. Chem. B* 119 (2015) 3499–3509.
- [29] M. Akram, I.A. Bhat, W.F. Bhat, Kabir-ud-Din, *Spectrochim. Acta A* 150 (2015) 440–450.
- [30] D. Mustard, D.W. Ritchie, *Proteins Struct. Funct. Bioinf.* 60 (2005) 269–274.
- [31] W.L. DeLano, *The PyMOL Molecular Graphics System*, DeLano Scientific, San Carlos, CA, USA, 2002.
- [32] P. Khullar, V. Singh, A. Mahal, H. Kumar, G. Kaur, M. Bakshi, *J. Phys. Chem. B* 117 (2013) 3028–3039.
- [33] N.A. Fazili, A. Naem, *Cell Biochem. Biophys.* 66 (2013) 265–275.
- [34] M. Amiri, K. Jankeje, J.R. Albani, *J. Fluoresc.* 20 (2010) 651–656.
- [35] Y. Ni, S. Wang, S. Kokot, *Anal. Chim. Acta* 663 (2010) 139–146.
- [36] V.I. Martín, A. Rodríguez, A. Maestre, M.L. Moya, *Langmuir* 29 (2013) 7629–7641.
- [37] M. Dockal, D.C. Carter, F. Rüker, *J. Biol. Chem.* 275 (2000) 3042–3050.
- [38] Y.H. Chen, J.T. Yang, H.M. Martinez, *Biochemistry* 11 (1972) 4120–4131.
- [39] X.L. Han, P. Mei, Y. Liu, Q. Xiao, F.L. Jiang, R. Li, *Spectrochim. Acta A* 74 (2009) 781–787.
- [40] X. Pan, R. Liu, P. Qin, L. Wang, X. Zhao, *J. Lumin.* 130 (2010) 611–617.
- [41] P.D. Ross, S. Subramanian, *Biochemistry* 20 (1981) 3096–3102.
- [42] J. Tian, J. Liu, Z. Hu, X. Chen, *Bioorg. Med. Chem.* 13 (2005) 4124–4129.
- [43] N.J. Faergeman, B.W. Sigurskjold, B.B. Kragelund, K.V. Andersen, J. Knudsen, *Biochemistry* 35 (1996) 14118–14126.
- [44] J. Rosendal, P. Ertbjerg, J. Knudsen, *Biochem. J.* 290 (1993) 316–321.
- [45] M. Akram, I.A. Bhat, Kabir-ud-Din, *Int. J. Biol. Macromol.* 78 (2015) 62–71.
- [46] P. Khullar, V. Singh, A. Mahal, P.N. Dave, S. Thakur, G. Kaur, J. Singh, S.S. Kamboj, M.S. Bakshi, *J. Phys. Chem. C* 116 (2012) 8834–8843.